

Coherent Control with User-Defined Passage

Bao-Jie Liu¹ and Man-Hong Yung^{1,2,3,4,*}

¹*Department of Physics, Southern University of Science and Technology, Shenzhen 518055, China*

²*Shenzhen Institute for Quantum Science and Engineering,*

Southern University of Science and Technology, Shenzhen 518055, China

³*Guangdong Provincial Key Laboratory of Quantum Science and Engineering,*
Southern University of Science and Technology, Shenzhen 518055, China

⁴*Shenzhen Key Laboratory of Quantum Science and Engineering,*
Southern University of Science and Technology, Shenzhen, 518055, China

(Dated: April 27, 2022)

Stimulated Raman adiabatic passage (STIRAP) is a standard technique in realizing robust quantum state control for many applications in physics, chemistry, and beyond, against experimental imperfections. However, STIRAP is susceptible to decoherence due to long evolution time. Here, we develop an alternative approach, termed stimulated Raman user-defined passage, called STIRUP, which allows users to design different fast and robust passages against both decoherence and imperfection. Comparing with shortcut to adiabaticity and its variants, this approach is simpler and more efficient to extend many-level and many-qubit system. Furthermore, STIRUP has many important physical applications such as geometric phase measurement, coherent population transfer, and quantum state preparation. Specifically, we can realize high-fidelity and robust state transfer and entangled state generation via STIRUP with state-of-the-art experimental implementations of superconducting circuits.

I. INTRODUCTION

Coherent control of quantum states is of fundamental importance to quantum information processing, such as high-precision sensing [1, 2], robust quantum computation [3, 4], and simulation [5]. There are a lot of quantum optimal control methods developed to realize high fidelity state preparations that are robust against decoherence and control parameter variations [6–14]. One of the more effective methods is the adiabatic control protocol, where control parameters are slowly changed to avoid transitions between different sets of eigenstates. In particular, stimulated Raman adiabatic passage (STIRAP) [13] based on the “adiabatic passage” without a lossy excited state has become a standard coherent control technique. STIRAP has two attractive properties [14] which are (i) robust against loss due to spontaneous emission from the loss excited state; (ii) robust against small variations of experimental control parameters, such as pulse amplitude, pulse timing and pulse phase. With these advantages, STIRAP has been proposed and demonstrated for realizing quantum state control [15] and for constructing holonomic quantum gates [16, 17]. However, these applications are limited by the intrinsic adiabatic condition, which implies lengthy evolution time; therefore STIRAP applications are still susceptible to the environment-induced decoherence [14], especially, dephasing error. More specifically, when dephasing errors have important effects on solid-state quantum systems such as superconducting circuit [18–21], quantum dot [22] and NV center in diamond [23], the effectiveness of STIRAP will be greatly reduced.

To overcome such a problem, we demonstrate that the notion of the adiabatic passage in STIRAP can be extended without the adiabatic condition. Specifically, we choose to

determine the driving pulses directly from the inverse engineering of some user-defined passage. We present a general scheme, stimulated Raman user-defined passage (STIRUP), which allows users to design fast and robust passages against the decay, dephasing and imperfection. Specifically, with the flexibility of STIRUP, one can optimize different objectives for different tasks, such as minimizing leakage error, enhancing robustness against control errors, speeding up quantum control. More importantly, our scheme can be regarded as a generalization of STIRAP and stimulated Raman shortcut-to-adiabatic passage (STIRSAP) [24–44], as it yields identical results to STIRAP in the adiabatic condition, as shown in Fig. (1a). Furthermore, our approach is more robust against decoherence than STIRAP, and is simpler and more efficient than STIRSAP for complex systems without relying on counteradiabatic driving [26–32], dynamical invariant [35–38] and dressed-state [39–41]. Finally, we apply STIRUP to an N-level pod (N-pod) system using state-of-the-art superconducting circuits experiment, we propose scenarios which implement robust many-qubit state transfer and entangled state generation.

II. GENERAL MODEL OF STIRUP

The family of quantum control problems investigated in this work is focused on the problems of preparing a certain N -dimensional target state $|\psi_T\rangle = \sum_{n=1}^N c_n |n\rangle$, starting from a given initial state $|\psi_0\rangle = \sum_{n=1}^N b_n |n\rangle$. One is required to find the corresponding driving Hamiltonian $H(t)$ for achieving such a goal. For this purpose, the term “passage” may be defined as a parameterized time-dependent state $|\phi_P(t)\rangle$ satisfying boundary conditions at time $t = 0$ and $t = T$: $|\phi_P(t=0)\rangle = |\psi_0\rangle$, and $|\phi_P(t=T)\rangle = |\psi_T\rangle$.

An example is the application of STIRAP on a three-level $\{|1\rangle, |2\rangle, |3\rangle\}$ lambda system [13–15]. The “adiabatic” pas-

* yung@sustech.edu.cn

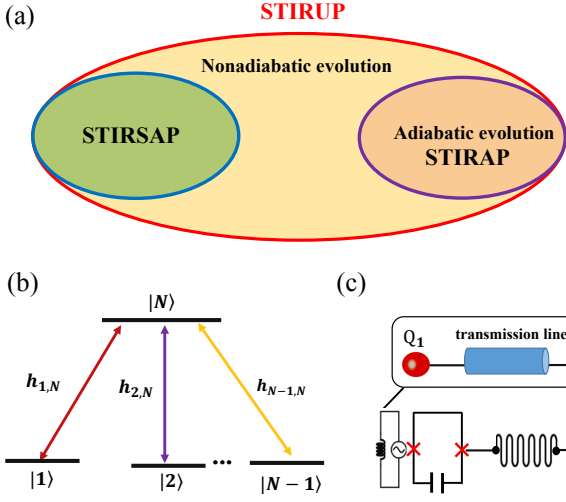


FIG. 1. The illustration of our proposed implementation. (a) Schematic of relations of known quantum control methods, STIR-SAP and STIRAP are included in STIRUP. (b) The N -pod level structure and coupling configuration. (c) Schematic of our circuit consisting of two capacitively coupled qubits, where Q2 is biased by an ac magnetic flux to periodically modulate its transition frequency. Q1 and Q2 are coupled via transmission-line-resonator.

sage is defined by $|\phi_A(t)\rangle \equiv \cos \theta(t)|1\rangle - \sin \theta(t)|2\rangle$, where $\theta(t)$ is required to satisfy the boundary conditions: $\theta(0) = 0$, and $\theta(T) = \pi/2$. In this way, one can achieve the goal of population transfer from $|1\rangle$ to $|3\rangle$. The passage is adiabatic because the strategy of STIRAP is based on the design of a driving Hamiltonian $H(t) = h_{13}(t)|1\rangle\langle 3| + h_{23}(t)|2\rangle\langle 3| + h.c.$, where the passage becomes an eigenstate of $H(t)$ when $\tan \theta(t) = h_{13}(t)/h_{23}(t)$. Then, it is sufficient to vary the driving amplitudes $\Omega_{0,1}$ sufficiently slowly compared with the energy gap.

However, the notion of the adiabatic passage in STIRAP can be extended without the adiabatic condition. Specifically, we choose to determine the driving pulses directly from the inverse engineering of some “user-defined” passage $|\phi_P(t)\rangle$. Without loss of generality, the user-defined” passage $|\phi_P(t)\rangle$ can be generally parameterized as

$$|\phi_P(t)\rangle = \sum_{n=1}^N a_n(t)|n\rangle, \quad (1)$$

where the time-dependent coefficients $a_n(t)$ satisfy boundary conditions $a_n(0) = b_n$, $a_n(T) = c_n$ and normalized condition $\sum_{n=1}^N |a_n(t)|^2 = 1$.

From the Schrödinger equation, the time dependence of the driving pulses are governed by the following set of equations, $\sum_n h_{mn}(t)a_n(t) = i\dot{a}_m(t)$. However, unlike the traditional approach of solving the Schrödinger equation, where the Hamiltonian is usually given, here both the matrix elements $h_{mn}(t) = \langle m|H(t)|n\rangle$, and the coefficients $a_n(t)$ have to be determined consistently. In general, one may reduce the degrees of freedom of the passage by requiring it to evolve along a certain pathway, and the Hamiltonian would naturally

has some physical constraints. Therefore, solving the set of coupled equations may not necessarily be a trivial task.

The point is that the state preparation problem constraints only the user-defined passage through the different boundary conditions, but the trajectory can be designed for optimizing additional objectives, such as noise robustness, decoherence errors, or time duration, as discussed below.

As a demonstration, we consider an N -level pod (N -pod) system with an N -dimensional state space, where a single level labeled $|N\rangle$ is coupled to $N-1$ levels labeled $|m\rangle$ ($m=1, \dots, N-1$) as shown in Fig. (1c). Previously, STIRAP was applied to 3-level systems [13] for realizing an efficient coherent population transfer via adiabatic passage $|\phi_A(t)\rangle$ from an initial state $|1\rangle$ to a target state $|3\rangle$, which is achieved by means of a two-photon process involving the driving pulses fields $h_{13}(t)$ and $h_{23}(t)$. Afterwards, STIRAP was extended to an N -pod system for realizing adiabatic population transfer [46, 47] and simulating non-Abelian gauge fields [48, 49]. Here, with essentially the same physical setting, we apply STIRUP pulses for quantum control of N -pod system, avoiding the adiabatic constraint.

The corresponding N -pod Hamiltonian $H_1(t)$, is described by [14]

$$H(t) = \sum_{m=0}^{N-1} \frac{\omega_{mN}}{2} \sigma_{z_m} + h_{mN}(t) \cos(\omega_{d_m} t) \sigma_{x_m} \quad (2)$$

where ω_{mN} is the energy splitting of the level $|m\rangle$ and $|N\rangle$, and $\sigma_{z_m} = |m\rangle\langle m| - |N\rangle\langle N|$ and $\sigma_{x_m} = |m\rangle\langle N| + |N\rangle\langle m|$ is the Pauli matrix defined by the ground state $|m\rangle$ level and excited level $|N\rangle$; and the control field $h_{mN}(t)$ drives the $|m\rangle \leftrightarrow |N\rangle$ transitions. When the two-photon resonant condition $\omega_{mN} = \omega_{d_m}$ is satisfied, under the rotating-wave approximation and the interaction picture, the system Hamiltonian can be written as,

$$H_I(t) = \sum_{m=1}^{N-1} h_{mN}(t) \sigma_{x_m}, \quad (3)$$

Here, our user-defined passage for a N -pod system can be parameterized as:

$$a_1 = \cos \gamma \prod_{i=1}^{N-2} \cos \chi_i, \quad a_{N-1} = -\cos \gamma \sin \chi_{N-2} \quad (4)$$

$$a_k = \cos \gamma \sin \chi_{k-1} \prod_{i=k}^{N-2} \cos \chi_i, \quad a_N = -i \sin \gamma.$$

where $\chi_i(t)$ and $\gamma(t)$ are generally time-dependent variables to be determined below with the integer k ranging from $k \in (1, N-1)$. To achieve state preparation from $|\phi_P(0)\rangle = |1\rangle$ to $|\phi_P(T)\rangle = |\psi_T\rangle$, it is sufficient to impose the following boundary conditions: $\gamma(0) = \gamma(T) = 0$, $\chi_i(0) = 0$ and $\chi_i(T) = s_i$.

Substituting Eq. (4) and Eq. (3) into the Schrödinger equa-

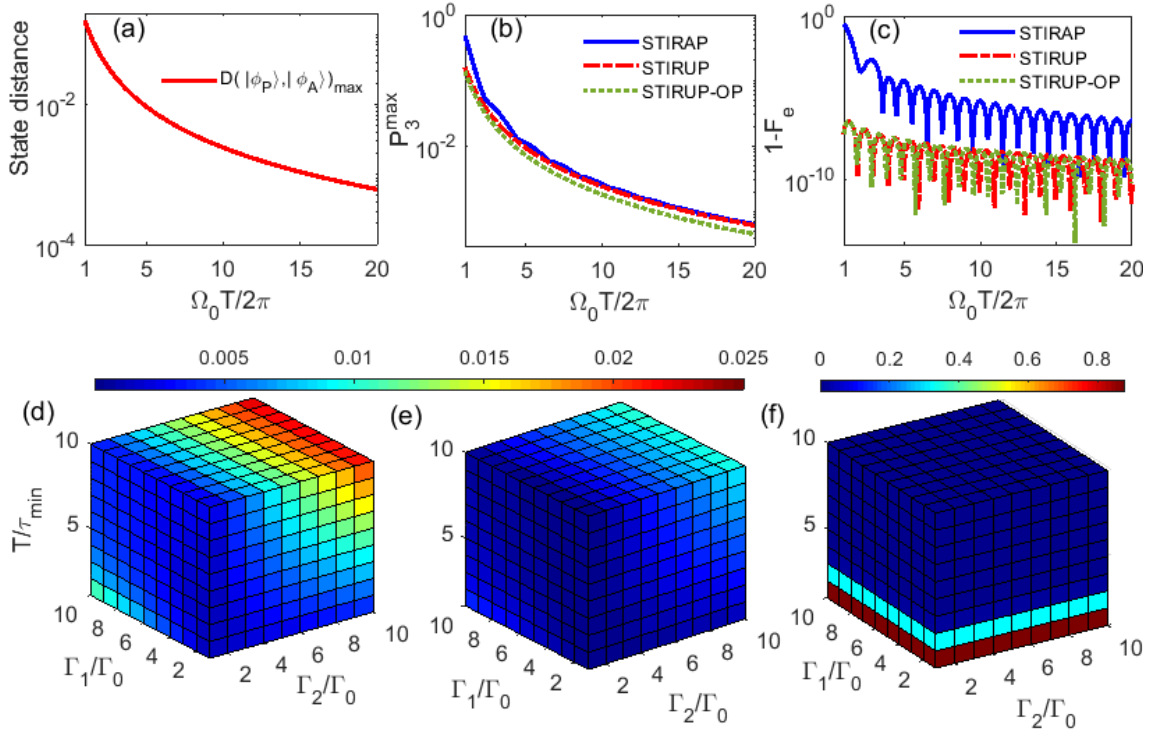


FIG. 2. (a) The maximum state distance between the user defined" passage $|\phi_P\rangle$ and the adiabatic passage $|\phi_A\rangle$ as a function of dimensionless parameter $\Omega_0 T$ (b) The maximum population P_3^{\max} in the intermediate level $|3\rangle$ of the STIRUP, STIRUP-OP and STIRAP. The error transfer efficiency of (d) STIRUP, (e) STIRUP-OP and (f) STIRAP as the functions of the decay rate Γ_1 , the dephasing rate Γ_2 and the evolution time T .

tion, the inverse engineering control fields is given by

$$\begin{aligned}
 h_{1N} &= f_1 \prod_{i=1}^{N-2} \cos \chi_i \\
 h_{kN} &= [f_k \sin \chi_{m-1} - \dot{\chi}_{m-1} \cos \chi_{m-1} \cot \gamma] \prod_{i=m}^{N-2} \cos \chi_i \\
 h_{N-1N} &= \dot{\chi}_{N-2} \cot \gamma \cos \chi_{N-2} - \dot{\gamma} \sin \chi_{N-2}
 \end{aligned} \tag{5}$$

where $f_x \equiv \left(\dot{\gamma} + \cot \gamma \sum_{l=x}^{N-2} \dot{\chi}_l \tan \chi_l \right)$. Note however that extra care must be taken at the initial time $t = 0$, as the boundary conditions would imply a divergence of the driving pulses whenever $\cot \gamma|_{\gamma \rightarrow 0} \rightarrow \infty$. To overcome such a problem, we enforce additional boundary conditions: $\dot{\chi}_m(0) = \dot{\chi}_m(T) = 0$, to maintain the combination $h_{mN}(t)$ to be finite.

Under the coupled differential equations in Eq. (5), we can realize arbitrary state preparation using our STIRUP by choosing proper boundary conditions. For example, to realize coherent population transfer from initial quantum state $|\psi_0\rangle = |1\rangle$ to the target state $|\psi_t\rangle = |N-1\rangle$, the boundary conditions are set to $\chi_i(T) = s_i = \pi/2$. One possible set of

solution is found to be

$$\begin{aligned}
 \gamma(t) &= \arctan \left[\frac{\dot{\chi}(t)}{\Omega_0} \right] \\
 \chi_i(t) &= \chi(t) = \arctan \left[\frac{1 - \cos(\pi t/T)}{1 + \cos(\pi t/T)} \right]
 \end{aligned} \tag{6}$$

where Ω_0 is a constant to control the pulse amplitude. Due to the flexibility of STIRUP, we can also set the parameter $\Omega_0 \rightarrow \Omega_0 \left[1 + Q \left(1 - \cos \frac{2\pi t}{T} \right)^4 \right]$ to reduce the population of intermediate level $|N\rangle$, where Q can be determined via numerical optimization. In this way, the time dependence of Rabi control pulses $h_{13}(t)$ and $h_{23}(t)$ can also be determined numerically.

More specifically, using the Eq. (4), the user-defined" passage is taken as $|\phi_P(t)\rangle = \cos \chi(t) \cos \gamma(t) |1\rangle - \sin \chi(t) \cos \gamma(t) |2\rangle - i \sin \gamma(t) |3\rangle$, which is corresponding to $a_1(t) = \cos \chi(t) \cos \gamma(t)$, $a_2(t) = \sin \chi(t) \cos \gamma(t)$ and $a_3(t) = -i \sin \gamma(t)$. Consequently, the time dependence of the control pulses can be determined by Eq. (5) as $h_{13}(t) = \dot{\chi} \cot \gamma \sin \chi(t) + \dot{\gamma}(t) \cos \chi(t)$ and $h_{23}(t) = \dot{\beta}(t) \cot \gamma(t) \cos \chi - \dot{\gamma}(t) \sin \chi(t)$. There, the nonadiabatic state transfer from $|1\rangle$ to $|3\rangle$ can be realized.

III. THE GENERALITY AND SUPERIORITY OF STIRUP

Here, we demonstrate that STIRUP is a general protocol that can reproduce the outcomes of all other methods by designing different passages, and take the STIRAP as an example. Before that, a minimum time τ_{min} of STIRUP is defined by the constraint that the STIRUP pulse cannot exceed its maximal amplitude of STIRAP at each moment, $\{h_{13}(t), h_{23}(t)\}_{STIRUP}^{\max} \leq \{h_{13}(t), h_{23}(t)\}_{STIRAP}^{\max}$, due to the limitation of experimental conditions. For the solution in Eq. (6), we numerically get $\tau_{min} = 3.24/\Omega_0$. When the above adiabatic condition is satisfied $|\dot{\theta}| \ll 1$, the dark state $|E_0(t)\rangle$ is an approximate solution of Schrödinger equation, i.e., $|E_0(t)\rangle = |\Phi_p(t)\rangle$. Therefore the STIRAP scheme can be viewed as one customized STIRUP passage under the adiabatic condition. To further illustrate it, we gradually increase the operation time T from $T = \tau_{min}$ to $T = 40\tau_{min}$ to be close to local adiabatic condition, where adiabatic condition is usually well satisfied under the condition, $\Omega_0 T > 2\pi \times 10$, obtained from experience and numerical simulation studies [13].

Here, we use the maximum state distance defined by $D(|\phi_P\rangle, |\phi_A\rangle)_{\max} = \frac{|T_r(|\phi_P\rangle\langle\phi_P| - |\phi_A\rangle\langle\phi_A|)_{\max}|}{2}$, to evaluate the gap between STIRAP and STIRUP. From the Fig. 2(a), the result can clearly verify our analysis that STIRUP gradually becomes STIRAP as the local adiabatic condition approaches. Comparison of the maximum population P_3^{\max} in the intermediate level $|3\rangle$ of the STIRUP to STIRAP, STIRUP has better performance than STIRAP regardless of whether the adiabatic condition is met as shown in Fig. 2(b). Furthermore, to further reduce the intermediate state occupation against decoherence, we can numerically design the optimal parameter Q as given by the Table I. In Fig. 2(d), we plot the error transfer efficiency $1 - F_e$ as a function of $\Omega_0 T$ for STIRAP, STIRUP and STIRUP-OP, where F_e is transfer efficiency defined by $F_e = |\langle\phi_P(T)|\psi_t\rangle|^2$. Comparing with STIRAP, both STIRUP and STIRAP reduce the error transfer efficiency by the same amount and lead to a several orders of magnitude reduction.

The decoherence process is unavoidable, and understanding its effects is crucial for quantum state control. The performance of STIRUP, STIRUP-OP and STIRAP can be simulated by using the Lindblad master equation [54]

$$\dot{\rho}(t) = i[\rho(t), H(t)] + \frac{\Gamma_1}{2}\mathcal{L}(S_-) + \frac{\Gamma_2}{2}\mathcal{L}(S_+), \quad (7)$$

where ρ is the density matrix of the considered system, $\mathcal{L}(A) = 2A\rho_1 A^\dagger - A^\dagger A\rho_1 - \rho_1 A^\dagger A$ is the Lindbladian of the operator A , $S_- = |1\rangle\langle 3| + |2\rangle\langle 3|$, $S_+ = |2\rangle\langle 2| + |3\rangle\langle 3|$; Γ_1 and Γ_2 are the decay and dephasing rates of the system, respectively. In our simulation, we plot the error transfer efficiency of STIRUP, STIRUP-OP and STIRAP with different the decoherence rates Γ_1 and Γ_2 with the unit of $\Gamma_0 = 2\pi \times 5$ kHz, and the different evolution time T as shown in Fig 4 (d-f). We can clearly see that Our STIRUP and STIRUP-OP model can give the optimal evolution time for different Γ_1 and Γ_2 of different experimental parameters, and STIRAP has an effect

only when Γ_1 is much larger than Γ_2 due to long evolution time.

TABLE I. Optimal pulses with the control parameters Q for different evolution time T .

T/τ_{min}	1	2	3	4	5	6	7	8	9
Q/100	2	1.58	1.37	1.26	1.2	1.16	1.14	1.12	1.11
T/τ_{min}	11	12	13	14	15	16	17	18-39	40
Q/100	1.09	1.09	1.09	1.08	1.08	1.08	1.08	1.07	1.06

IV. APPLICATION OF STIRUP ON SUPERCONDUCTING CIRCUITS

In this part, we will make our discussion explicit by demonstrating its application in realistic systems, namely, superconducting circuits. Specifically, we shall focus on a many-qubit superconducting quantum processor in Ref. [50–52], as shown in Fig. 1(d). All qubits are interconnected by a central cavity (bus resonator), and the frequency of each qubit can be individually manipulated with its control lines. In the rotating wave approximation and ignoring the cross talk between qubits, we can describe this system using a Tavis-Cummings model [53] and write the Hamiltonian of the system as

$$H_3(t) = \omega_c a^\dagger a + \sum_{j=0}^{N-1} \left[\frac{\omega_{q_j}}{2} \sigma_j^z + g_j (\sigma_j^+ a + \sigma_j^- a^\dagger) \right], \quad (8)$$

where ω_c is the frequency of cavity, ω_{q_j} is the energy splitting of the qubit, σ_j^z is the Pauli matrix of the j th qubit in its eigenbasis, g is the qubit-cavity coupling strength, σ_j (σ_j^+) is the qubit lower (raising) operator, and a^\dagger (a) is the creation (annihilation) operator of cavity. To obtain tunable coupling between the two qubits, we add an ac magnetic flux on the j th qubit to periodically modulate its frequency as $\omega_{q_2}(t) = \omega_{q_2} + \varepsilon_j(t) \cos(\nu_j t)$, where $\varepsilon_j(t)$, and ν_j are the modulation amplitude, and frequency, respectively. Moving into the interaction picture, the effective interaction Hamiltonian is

$$H_4(t) = \sum_{j=0}^{N-1} \tilde{g}_j(t) (\sigma_j^+ a + \sigma_j^- a^\dagger). \quad (9)$$

where the time-dependent effective coupling is $\tilde{g}_j(t) = g_j J_1(\varepsilon_j(t))$, and J_1 is the Bessel function.

Here, we firstly demonstrate the state transfer from the initial state $|eg0\rangle$ to the target state $|ge0\rangle$ in superconducting quantum processor. In a single-excitation subspace spanned by $\{|eg0\rangle, |ge0\rangle, |gg1\rangle\}$, denoting the states of qubits and the cavity, the Hamiltonian Eq. (9) has the same form as the Eq. (3) of N-pod system corresponding to $N=4$.

As shown in Fig. 1(c), for the tripod system with $N=3$

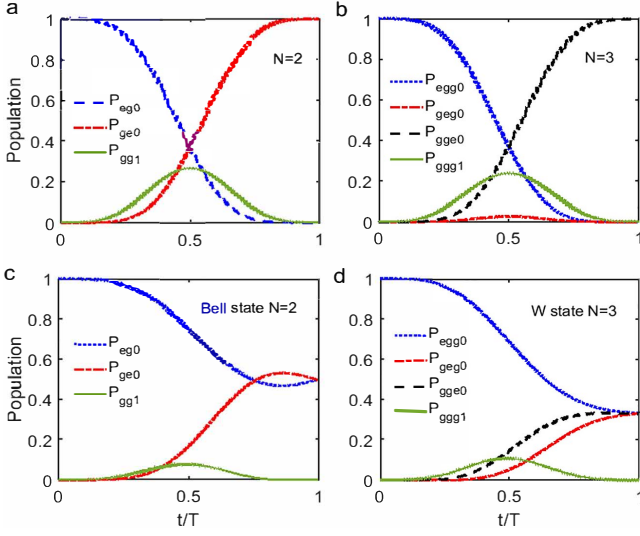


FIG. 3. (a) The dynamical population of two-qubit and three-qubit QST, and the dynamical population of Bell state and W state via STIRUP.

($j=3$), the passage is chosen as

$$|\phi_t(t)\rangle = \cos \beta_1 \cos \gamma_1 \cos \phi_1 |egg0\rangle + \sin \beta_1 \cos \gamma_1 |gge0\rangle + \cos \beta_1 \cos \gamma_1 \sin \phi_1 |geg0\rangle - i \sin \gamma_1 |ggg1\rangle \quad (10)$$

The boundary condition of β_1 and γ_1 is the same as β_0 and γ_0 for the case $N=2$. In addition, the control parameter ϕ_1 satisfies the condition $\phi_1(0) = 0(\pi)$, the corresponding solution is given by $\beta_1(t) = \beta_0$, $\gamma_1(t) = \gamma_0$, and $\phi_1(t) = \arctan\left(\frac{\cos \beta_0 \cos \gamma_0 - 1}{\cos \beta_0 \cos \gamma_0 + 1}\right)$. According to the Eq. (5), we get the Rabi pulse shapes of $\tilde{g}_0(t)$, $\tilde{g}_1(t)$ and $\tilde{g}_2(t)$. Therefore, the high-fidelity QST can be realized from the initial state $|egg0\rangle$ to the target state $|gge0\rangle$.

Numerical simulation of the QST population dynamics are shown in Fig. (3a) and (3b), where the high-fidelity QST fidelities of for the three-qubit and four-qubit QST can be obtained with 99.4% and 99.19% using the following set of the current experimental parameters [55–57]: the cavity and qubit frequency is $\nu_j = \omega_c - \omega_{q_j} = 2\pi \times 1$ GHz, the gate time is set $T = 82$ ns, and the dissipation parameters of the cavity and qubits are taken $\Gamma_c = 2\pi \times 5$ kHz.

Secondly, we can realize a high-fidelity entangled state preparation via one-step STIRUP. To generate two-qubit Bell state $|\Psi_B\rangle = \frac{|eg\rangle + |eg\rangle}{\sqrt{2}}$, the boundary conditions are setted as $\gamma_0(0) = \gamma_0(T) = 0(\pi)$ and $\beta_0(0) = 0$, $\beta_0(T) = \pi/4$, with the corresponding parameters $\beta(t) = \frac{\pi t}{2T}$ and $T = 90$ ns. As shown in Fig. (3c), with the numerical simulation, the Bell state is formed with fidelity as high as 99.7% due to loss excited state $|gg1\rangle$ population and short-time evolution. To further improve the fidelity, we can combine STIRUP with the quantum optimal control pulse to minimize the effect of higher levels. Similar to the approach of generating Bell state, the tripartite entanglement W state $|\Psi_w\rangle = \frac{|egg\rangle + |geg\rangle + |gge\rangle}{\sqrt{3}}$ can be generated by choosing $j = 3$, $\beta(t) = S_1 t/T$, $\gamma_1 =$

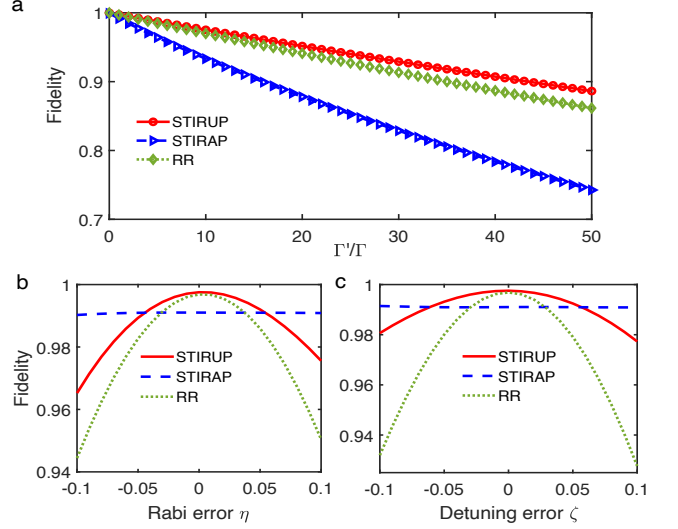


FIG. 4. (a) The two-qubit QST fidelities of STIRUP, STIRAP and Rabi Resonate (RR) as a function of (a) decoherence rates Γ' (in unit of Γ), (b) Rabi error η and detuning error ζ .

$1/\sqrt{3} \sin S_1$ and $T = 98.5$ ns with $S_1 = 0.5678\pi$. As shown in Fig. (3d), the W state $|\Psi_w\rangle$ can be achieved with high fidelity 98.4%. The genuine entanglement states of Bell state and W state violate entanglement witnesses that rule out bi-separability, have been generated. This ability to couple three-qubit system and create entangled states which are qualitatively different is a significant step towards salable quantum information processing with superconducting devices.

V. ROBUSTNESS

We proceed to show the superiority of STIRUP on robustness against environmental noises and experimental imperfections. Firstly, to investigate the robustness against decoherence comparing with STIRAP [63] and resonate Rabi pulses (RR) in Ref. [64–67] in a three-state system. We plot the QST fidelity defined by $F = |\langle \phi_I | \phi_t(T) \rangle|^2$ as functions of the decoherence rate Γ' (in unit of Γ), where $|\phi_I\rangle$ represents the ideal target state for STIRUP, STIRAP, and RR schemes, as shown in Fig. (4a). Clearly, STIRUP is more robust against the decoherence effect comparing with STIRAP and RR schemes due to its' short evolution time and loss excited-state population.

Secondly, to test the robustness of STIRUP against experimental pulse errors caused by an usual slow quasistatic noise, we add a static deviation to the strength of driving pulse, i.e., $\tilde{g}_{max} \rightarrow (1 + \eta)\tilde{g}_{max}$, where $\eta \in [-0.1, 0.1]$ represents the Rabi error. In other words, the Hamiltonian becomes $H_3(t) \rightarrow (1 + \eta)H_3(t)$. Comparing our STIRUP with the STIRAP and RR methods, we simulated the performance of QST with the same pulse error under the decoherence effect. As shown in Fig. (4b), STIRUP is not only always more robust than the STIRAP scheme but also RR scheme when the Rabi error is small. Finally, we further investigate the sensitivity of

the STIRUP protocol to the variation of the qubit frequency detuning $\omega_{q_j} \rightarrow \omega_{q_j} + \delta$, where we denote the detuning error as $\delta = \zeta \tilde{g}_{max}$ with $\zeta \in [-0.1, 0.1]$. As shown in Fig. (4c), the transfer fidelity of STIRUP is also more robust against the detuning error ζ than others within the small detuning error.

VI. CONCLUSION

We have presented a scheme that allows users to design different fast and robust passages against both decoherence and imperfection by directly engineering solutions of the Schrödinger equation. Consequently, this approach is simpler and more efficient when extending to many-level and many-qubit system comparing with shortcuts to adiabaticity. Furthermore, STIRUP has many important physical applications such as geometric quantum computation, coherent population transfer, and quantum state preparation. Specifically, we realized many-level state transfer and many-qubit entangled state

generation with high fidelity and noise robustness by using STIRUP.

ACKNOWLEDGMENTS

This work is supported by the Natural Science Foundation of Guangdong Province (Grant No. 2017B030308003), the Key R & D Program of Guangdong province (Grant No. 2018B030326001), the Science, Technology and Innovation Commission of Shenzhen Municipality (Grant No. JCYJ20170412152620376 and No. JCYJ20170817105046702 and No. KYT-DPT20181011104202253), National Natural Science Foundation of China (Grant No. 11875160 and No. U1801661), the Economy, Trade and Information Commission of Shenzhen Municipality (Grant No. 201901161512), Guangdong Provincial Key Laboratory (Grant No. 2019B121203002).

-
- [1] M. Kasevich, Coherence with atoms, *Science* **298**, 13631368 (2002).
 - [2] K. Kotru, D. L. Butts, J. M. Kinast, and R. E. Stoner, Large-area atom interferometry with frequency-swept Raman adiabatic passage, *Phys. Rev. Lett.* **115**, 103001 (2015).
 - [3] E. Farhi, J. Goldstone, S. Gutmann, J. Lapan, A. Lundgren, and D. Preda, A quantum adiabatic evolution algorithm applied to random instances of an NP-complete problem, *Science* **292**, 472475 (2001).
 - [4] C. Monroe, and J. Kim, Scaling the ion trap quantum processor, *Science* **339**, 11641169 (2013).
 - [5] K. Kim, M.-S. Chang, S. Korenblit, R. Islam, E. E. Edwards, J. K. Freericks, G.-D. Lin, L.-M. Duan, and C. Monroe, Quantum simulation of frustrated Ising spins with trapped ions, *Nature* **465**, 590-593 (2010).
 - [6] K. Khodjasteh, and D. A. Lidar, Fault-Tolerant Quantum Dynamical Decoupling, *Phys. Rev. Lett.* **95**, 180501 (2005).
 - [7] A. M. Souza, G. A. Alvarez, and D. Suter, Robust Dynamical Decoupling for Quantum Computing and Quantum Memory, *Phys. Rev. Lett.* **106**, 240501 (2011).
 - [8] G. T. Genov, D. Schraft, N. V. Vitanov, and T. Halfmann, Arbitrarily Accurate Pulse Sequences for Robust Dynamical Decoupling, *Phys. Rev. Lett.* **118**, 133202 (2017).
 - [9] K. Khodjasteh, and L. Viola, Dynamically Error-Corrected Gates for Universal Quantum Computation, *Phys. Rev. Lett.* **102**, 080501 (2009).
 - [10] X. Wang, L. S. Bishop, J. P. Kestner, E. Barnes, K. Sun, and S. D. Sarma, Composite pulses for robust universal control of singlet-triplet qubits, *Nat. Commun.* **3**, 997 (2012).
 - [11] X. Rong, J. Geng, F. Shi, Y. Liu, K. Xu, W. Ma, F. Kong, Z. Jiang, Y. Wu, and J. Du, Experimental fault-tolerant universal quantum gates with solid-state spins under ambient conditions, *Nat. Commun.* **6** (2015).
 - [12] G. S. Vasilev, A. Kuhn, and N. V. Vitanov, Optimum pulse shapes for stimulated Raman adiabatic passage, *Phys. Rev. A* **80**, 013417 (2009).
 - [13] K. Bergmann, H. Theuer, and B. W. Shore, Coherent population transfer among quantum states of atoms and molecules, *Rev. Mod. Phys.* **70**, 1003 (1998).
 - [14] N. V. Vitanov, A. A. Rangelov, B. W. Shore, and K. Bergmann, Stimulated Raman adiabatic passage in physics, chemistry, and beyond, *Rev. Mod. Phys.* **89**, 015006 (2017).
 - [15] K. Bergmann et al., Roadmap on STIRAP applications, *J. Phys. B: At. Mol. Opt. Phys.* **52**, 202001 (2019).
 - [16] P. Zanardi, and M. Rasetti, Holonomic quantum computation, *Phys. Lett. A* **264**, 94 (1999).
 - [17] L. M. Duan, J. I. Cirac, and P. Zoller, Geometric manipulation of trapped ions for quantum computation, *Science* **292**, 1695 (2001).
 - [18] S. P. Premaratne, F. C. Wellstood, and B. S. Palmer, Microwave photon Fock state generation by stimulated Raman adiabatic passage, *Nat. Commun.* **8**, 14148 (2017).
 - [19] K. S. Kumar, A. Vepsäläinen, S. Danilin, and G. S. Paraoanu, Stimulated Raman adiabatic passage in a three-level superconducting circuit, *Nat. Commun.* **7**, 10628 (2016).
 - [20] H. K. Xu, C. Song, W. Y. Liu, G. M. Xue, F. F. Su, H. Deng, Y. Tian, D. N. Zheng, S. Han, Y. P. Zhong, H. Wang, Y.-x. Liu, and S. P. Zhao, Coherent population transfer between uncoupled or weakly coupled states in ladder-type superconducting qutrits, *Nat. Commun.* **7**, 11018 (2016).
 - [21] A. Vepsäläinen, S. Danilin, S. Paraoanu, Superadiabatic population transfer in a three-level superconducting circuit, *Sci. Adv.* **5**, eaau5999 (2019).
 - [22] T. S. Koh, S. N. Coppersmith, and M. Friesen, High-fidelity gates in quantum dot spin qubits, *Proc Natl Acad Sci.* **110**, 1969519700 (2013).
 - [23] M. G. Bason, M. Viteau, N. Malossi, P. Huillery, E. Arimondo, D. Ciampini, R. Fazio, V. Giovannetti, R. Mannella, and O. Morsch, High-fidelity quantum driving, *Nature Phys.* **8**, 147 (2012).
 - [24] Torrontegui, E., S. Ibáñez, S. Martínez-Garaot, M. Modugno, A. del Campo, D. Guéry-Odelin, A. Ruschhaupt, X. Chen, and J. G. Muga, Shortcuts to adiabaticity, *Adv. At. Mol. Opt. Phys.* **62**, 117 (2013).
 - [25] D. Guéry-Odelin, A. Ruschhaupt, A. Kiely, E. Torrontegui, S. Martínez-Garaot, and J. G. Muga, Shortcuts to adiabaticity: concepts, methods, and applications, *Rev. Mod. Phys.* **91**, 045001 (2019).

- [26] R. G. Unanyan, L. P. Yatsenko, K. Bergmann, and B. W. Shore, Laser-induced adiabatic atomic reorientation with control of diabatic losses, *Opt. Comm.* **139**, 48 (1997)
- [27] A. Emmanouilidou, X.-G. Zhao, P. Ao, and Q. Niu, Steering an eigenstate to a destination, *Phys. Rev. Lett.* **85**, 1626 (2000).
- [28] M. Demirplak and S. A. Rice, Adiabatic population transfer with control fields, *J. Phys. Chem. A* **107**, 9937 (2003).
- [29] M. Demirplak and S. A. Rice, Assisted adiabatic passage revisited, *J. Phys. Chem. B* **109**, 6838 (2005).
- [30] M. Demirplak and S. A. Rice, Adiabatic population transfer with control fields, *J. Chem. Phys.* **129**, 154111, 6838 (2008).
- [31] M. V. Berry, Transitionless quantum driving, *J. Phys. A: Math. Theor.* **42**, 365303 (2009).
- [32] X. Chen, I. Lizuaín, A. Ruschhaupt, D. Guéry-Odelin, and J. G. Muga, Shortcut to adiabatic passage in two-and three-level atoms, *Phys. Rev. Lett.* **105**, 123003 (2010).
- [33] X.-K. Song, Q. Ai, J. Qiu, and F.-G. Deng, Physically feasible three-level transitionless quantum driving with multiple Schrödinger dynamics, *Phys. Rev. A* **93**, 052324 (2016).
- [34] Y. X. Du, Z. T. Liang, Y. C. Li, X. X. Yue, Q. X. Lv, W. Huang, X. Chen, H. Yan, and S. L. Zhu, Experimental realization of stimulated Raman shortcut-to-adiabatic passage with cold atoms, *Nat. Commun.* **7**, 12479 (2016).
- [35] H. R. Lewis, and W. B. Riesenfeld, An exact quantum theory of the time-dependent harmonic oscillator and of a charged particle in a time-dependent electromagnetic field, *J. Math. Phys.* **10**, 1458 (1969).
- [36] Xi Chen, E. Torrontegui, and J. G. Muga, Lewis-Riesenfeld invariants and transitionless quantum driving, *Phys. Rev. A* **83**, 062116 (2011).
- [37] X. Laforgue, X. Chen, and S. Guérin, Robust stimulated Raman exact passage using shaped pulses, *Phys. Rev. A* **100**, 023415 (2019).
- [38] T.-N. Xu, K. Liu, X. Chen, and S. Guérin, Invariant-based optimal composite stimulated Raman exact passage, *J. Phys. B: At. Mol. Opt. Phys.* **52**, 235501 (2019).
- [39] A. Baksic, H. Ribeiro, and A. A. Clerk, Speeding up adiabatic quantum state transfer by using dressed states, *Phys. Rev. Lett.* **116**, 230503 (2016).
- [40] B. B. Zhou, A. Baksic, H. Ribeiro, C. G. Yale, F. J. Heremans, P. C. Jerger, A. Auer, G. Burkard, A. A. Clerk, and D. D. Awschalom, Accelerated quantum control using superadiabatic dynamics in a solid-state lambda system, *Nat. Phys.* **13**, 330 (2017).
- [41] B.-H. Huang, Y.-H. Kang, Y.-H. Chen, Q.-C. Wu, J. Song, and Y. Xia, Fast quantum state engineering via universal SU (2) transformation, *Phys. Rev. A* **96**, 022314 (2017).
- [42] B.-J. Liu, X.-K. Song, Z.-Y. Xue, X. Wang, and M.-H. Yung, Plug-and-Play Approach to Nonadiabatic Geometric Quantum Gates, *Phys. Rev. Lett.* **123**, 100501 (2019).
- [43] T. Yan, B.-J. Liu, K. Xu, C. Song, S. Liu, Z. Zhang, H. Deng, Z. Yan, H. Rong, K. Huang, M.-H. Yung, Y. Chen, and D. Yu, Experimental Realization of Nonadiabatic Shortcut to Non-Abelian Geometric Gates, *Phys. Rev. Lett.* **122**, 080501 (2019).
- [44] V. Dorier, M. Gevorgyan, A. Ishkhanyan, C. Leroy, H. R. Jauslin, and S. Guérin, Nonlinear Stimulated Raman Exact Passage by Resonance-Locked Inverse Engineering, *Phys. Rev. Lett.* **119**, 243902 (2017).
- [45] M. Christandl, N. Datta, A. Ekert, and A. J. Landahl, Perfect state transfer in quantum spin networks, *Phys. Rev. Lett.* **92**, 187902 (2004).
- [46] P. A. Ivanov, E. S. Kyoseva, and N. V. Vitanov, Engineering of arbitrary U(N) transformations by quantum Householder reflections, *Phys. Rev. A*, **74**, 022323 (2006).
- [47] M. Amniet-Talab, M. Saadati-Niari, S. Guérin, and R. Nader-Ali, Superposition of states by adiabatic passage in N-pod systems, *Phys. Rev. A* **83**, 013817 (2011).
- [48] J. Dalibard, F. Gerbier, G. Juzeliūnas, and P. Ohberg, Colloquium: Artificial gauge potentials for neutral atom, *Rev. Mod. Phys.* **83**, 1523 (2011).
- [49] R. Barnett, G. R. Boyd, and V. Galitski, SU(3) Spin-Orbit Coupling in Systems of Ultracold Atoms, *Phys. Rev. Lett.* **109**, 235308 (2012)
- [50] C. Song, K. Xu, W. X. Liu, C. P. Yang, S. B. Zheng, H. Deng, Q. W. Xie, K. Q. Huang, Q. J. Guo, L. B. Zhang, P. F. Zhang, D. Xu, D. N. Zheng, X. B. Zhu, H. Wang, Y. A. Chen, C. Y. Lu, S. Y. Han, and J. W. Pan, 10-qubit entanglement and parallel logic operations with a superconducting circuit, *Phys. Rev. Lett.* **119**, 180511 (2017).
- [51] K. Xu, J. J. Chen, Y. Zeng, Y. R. Zhang, C. Song, W. X. Liu, Q. J. Guo, P. F. Zhang, D. Xu, H. Deng, K. Q. Huang, H. Wang, X. B. Zhu, D. N. Zheng, and H. Fan, Emulating many-body localization with a superconducting quantum processor, *Phys. Rev. Lett.* **120**, 050507 (2018).
- [52] C. Song, K. Xu, H. Li, Y. Zhang, X. Zhang, W. Liu, Q. Guo, Z. Wang, W. Ren, J. Hao, H. Feng, H. Fan, D. Zheng, D. Wang, H. Wang, and S. Zhu, Generation of multicomponent atomic Schrödinger cat states of up to 20 qubits, *Science* **365**, 574577 (2019)
- [53] M. Tavis, and F. W. Cummings, Exact Solution for an N-Molecule Radiation-Field Hamiltonian, *Phys. Rev.* **170**, 379 (1968).
- [54] G. Lindblad, On the generators of quantum dynamical semigroups, *Commun. Math. Phys.* **48**, 119130 (1976).
- [55] R. Barends, J. Kelly, A. Megrant, D. Sank, E. Jeffrey, Y. Chen, Y. Yin, B. Chiaro, J. Mutus, C. Neill, P. O'Malley, P. Roushan, J. Wenner, T. C. White, A. N. Cleland, and J. M. Martinis, Coherent Josephson qubit suitable for scalable quantum integrated circuits, *Phys. Rev. Lett.* **111**, 080502 (2013).
- [56] R. Barends, J. Kelly, A. Megrant, A. Veitia, D. Sank, E. Jeffrey, T. C. White, J. Mutus, A. G. Fowler, B. Campbell et al., Superconducting quantum circuits at the surface code threshold for fault tolerance, *Nature (London)* **508**, 500 (2014).
- [57] Z. Chen, J. Kelly, C. Quintana, R. Barends, B. Campbell, Y. Chen, B. Chiaro, A. Dunsworth, A. G. Fowler, E. Lucero et al., Measuring and suppressing quantum state leakage in a superconducting qubit, *Phys. Rev. Lett.* **116**, 020501 (2016).
- [58] F. Motzoi, J. M. Gambetta, P. Rebentrost, and F. K. Wilhelm, Simple Pulses for Elimination of Leakage in Weakly Nonlinear Qubits, *Phys. Rev. Lett.* **103**, 110501 (2009).
- [59] M. Neeley, R. C. Bialczak, M. Lenander, E. Lucero, M. Mariantoni, A. D. O'Connell, D. Sank, H. Wang, M. Weides, J. Wenner, Y. Yin, T. Yamamoto, A. N. Cleland, and J. M. Martinis, Generation of three-qubit entangled states using superconducting phase qubits, *Nature (London)* **467**, 570 (2010).
- [60] L. DiCarlo, M. D. Reed, L. Sun, B. R. Johnson, J. M. Chow, J. M. Gambetta, L. Frunzio, S. M. Girvin, M. H. Devoret, and R. J. Schoelkopf, Preparation and measurement of three-qubit entanglement in a superconducting circuit, *Nature (London)* **467**, 574 (2010).
- [61] F. Altomare, J. I. Park, K. Cicak, M. A. Sillanpää, M. S. Allman, D. Li, A. Sirois, J. A. Strong, J. D. Whittaker, and R. W. Simmonds, Tripartite interactions between two phase qubits and a resonant cavity, *Nat. Phys.* **6**, 777 (2010).
- [62] Erik Lucero, R. Barends, Y. Chen, J. Kelly, M. Mariantoni, A. Megrant, P. O'Malley, D. Sank, A. Vainsencher, J. Wenner, T. White, Y. Yin, A. N. Cleland, and John M. Martinis, Computing prime factors with a Josephson phase qubit quantum processor,

- Nat. Phys. **8**, 719 (2012).
- [63] H.-S. Chang, Y. P. Zhong, A. Bienfait, M.-H. Chou, C. R. Conner, É. Dumur, J. Grebel, G. A. Peairs, R. G. Povey K. J. Satzinger, and A. N. Cleland, Phys. Rev. Lett. **124**, 240502 (2020).
 - [64] J. A. Mlynek, A. A. Abdumalikov, Jr., J. M. Fink, L. Steffen, M. Baur, C. Lang, A. F. van Loo, and A. Wallraff, Demonstrating W-type entanglement of Dicke states in resonant cavity quantum electrodynamics, Phys. Rev. A **86**, 053838 (2012).
 - [65] R. J. Chapman, M. Santandrea, Z. Huang, G. Corrielli, A. Crespi, M.-H. Yung, R. Osellame, and A. Peruzzo, Experimental perfect state transfer of an entangled photonic qubit, Nat. Commun. **7**, 11339 (2016).
 - [66] D. J. Egger, M. Ganzhorn, G. Salis, A. Fuhrer, P. Müller, P. Kl. Barkoutsos, N. Moll, I. Tavernelli, and S. Filipp, Entanglement generation in superconducting qubits using holonomic operations, Phys. Rev. Applied **11**, 014017 (2019).
 - [67] X. Li, Y. Ma, J. Han, T. Chen, Y. Xu, W. Cai, H. Wang, Y.P. Song, Z.-Y. Xue, Z.-q. Yin, and L. Sun, Perfect quantum state transfer in a superconducting qubit chain with parametrically tunable couplings, Phys. Rev. Applied **10**, 054009 (2018).